Doppler-Free Saturation Spectroscopy

James Rizzardi, Ramil Aleskerov
(Dated: December 6, 2019)

The purpose of this experiment is to investigate the fine and hyperfine splitting within isotopic ^{87}Rb, and ^{85}Rb D2 lines. The experiment will be completed via demonstrating doppler-free saturation spectroscopy, and divided into multiple sections as an effort to exercise experimenters with the equipment. First and foremost, after having become familiarized with the equipment, experimenters will determine the laser output to be used later in the experiment, followed by the quantum efficiency of the cell. Experimenters will next attempt to present both a non-saturated, and a saturated spectrum provided by the Rb when exposed to the exciting IR laser as a function of wavelength.

I. INTRODUCTION

A. Background

Discovered in 1861 and reserving one of the most active positions in the periodic table, rubidium is known for having a "convenient" spectral absorption range, demonstrating Feshbach resonance at select frequencies. Further, with only a single electron in the ground state maintaining at $5^2S_{1/2}$, and excited state maintaining at $5^2P_{1/2,3/2}$, an unsaturated demonstration of the substance as a vapor can easily be observed. [1]

Fast forward a century, with the invention of the tunable lasers, the field of precision spectroscopy grew, also appending to our understanding of the atomic physics. As the name implies, spectroscopy can easily be described as an in depth analysis of the interaction between light, and some material substance. In the present case, tuned correctly, the monochromatic light from the laser will act as a resonant oscillatory source on the substance. If provided with an adequate intensity, free atoms will be forced into an excited (albeit, unstable) state. During this transition, a photon will be released, which can be absorbed with adequate photography tools (a camera capable of capturing the photon at the given frequency) In this case, with Rb: infrared. Further, if a photodiode is put in place to observe the laser intensity passing through or reflecting off the substance, one can observe the real time decrease in passing light, as the intersecting substance absorbs the light. This absorption will be the key measurement experimenters will observe, as each transition will provide a "fingerprint" detailing the fine and hyperfine splittings between transition states. [2]

1. *Doppler Broadening, and The Importance of "Doppler Free"*

The rubidium sample to be analyzed within this experiment will be a small glass cell, containing the substance as a vapor; this should immediately imply to any physics experimenter, there is going to be a maxwellian distribution in velocities within the cell. With this being said, any attempt to obtain a measurement will land experimenters in an imprecise distribution of temperatures, with a width proportional to mean the kinetic energy [3]. This drastically decreases the overall resolution of the experiment, providing far less significant results.

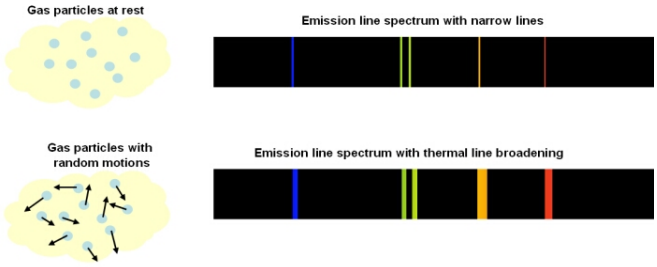

FIG. 1. Difference in emission lines with (bottom), and without(top) doppler broadening due to thermal motion. Observe the decrease in line width when thermal motion is minimized. Source: [3]

One solution to decrease the width of the distribution would be to cool the substance, observing the central narrowing of the width, and drawing a function to minimize the broadened range. However, a second solution using stimulated emission could be used, where a high and low intensity ("pump," and "probe" beam, respectively) laser of the same frequency is passed through the sample, using the setup mentioned in the previous section. Considering the difficulty in fine tuning a pair of lasers to be of the exact same frequency, the same laser will be used for both beams, after being passed through a beam splitter. When peak resonance is reached, the distribution of interacting atoms is minimized, depleting the distribution of doppler broadening. [2][3]

II. EXPERIMENTAL SETUP

As mentioned previously, in order to examine the hyperfine splittings with reasonable resolution beyond the doppler limit, it is important for the experiment to have easily controllable parameters, without modifying the laser except where need be. The apparatus will require two distinct "modes" of operation - one being saturated, the other unsaturated. Both modes of operation will utilize the same beam travel, with the single exception

that being the mode of saturation will have an additional probe beam (to be the "pump" beam) through the rubidium cell.

A. Laser Setup

The laser to be utilized in the experiment will be a current regulated 780nm distributed feedback laser, controlled up to 120mA. Laser output will passed through lens pair with an attenuator in between, to properly control beam divergence. These parameters will be pre-adjusted, and should not need adjusting during the experiment. Following, the beam will pass through a beam splitter, allowing the beam to be measured synchronously via a scanning Fabry-Perot interferometers. The primary beam will proceed through the Rb cell to be interpreted by a photo-diode, whose signal will be interpreted by oscilloscope. In front of the photodiode will be a mirror, allowing only 1% of light to be passed through - the rest, reflected back through the Rb cell. Under saturated conditions, the primary beam will follow to be split, and pass through the Rb cell in an opposite direction. Considering the intensity and direction of this beam, it is known as the "pump" beam, and key to exciting the vapor cell. A breakdown route for the laser is presented in Fig. 2.

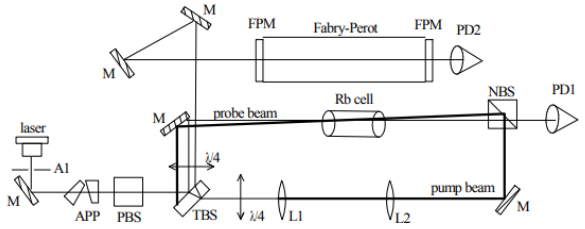

FIG. 2. Laser path setup including mirrors (M), various beam splitter (*BS), and Fabry-Perot interferometer ("fabry-perot mirror, FPM), Source: [4]

B. Fabry-Perot Interferometer

An essential, yet not previously mentioned, part of the experiment in order to get the incredibly high frequency results is a carefully tuned fabry-perot interferometer (FPI). The particular FPI to be used in the experiment is tuned with a finesse of 150, with a free spectral range of 10GHz. Prior to the laser being utilized to pass through the Rb cell, the laser will be passed through a beam splitter, with the unmentioned beam feeding toward the FPI. The advantage of using the FPI, is it allows experimenters to interpret collected data in terms of $sec^{-}1$. Figure 3 provides a sample of the signal to be interpreted on the oscilloscope. Distance between heightened peaks provides the time sampling with the known FSR. This is used extensively during interpretation of measurements, with the true collected sample displayed in figure 5.

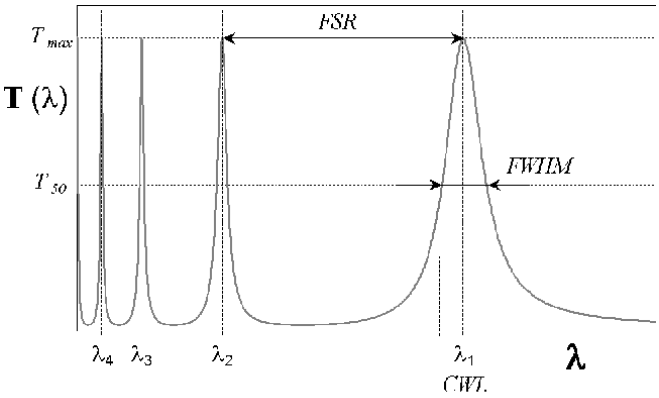

Fig. 2: Airy-function over wavelength

FIG. 3. Using interpreted FPI signal to interpret results in terms of frequency. With a known FSR, frequency can be calibrated to sampling on the oscilloscope. Source: [5]

III. THEORY

As mentioned previously, there has been extensive documentation on each of the components to be observed throughout the experiment. However, we must proceed with the notion of confirming existing knowledge. Firstly, it is important to emphasize on the likelihood experimenters will observe spontaneous emission within the cell.

Upon reaching resonant frequencies, it is expected the laser will stimulate emission of the Rb, visible in all directions within the IR spectra. Upon reaching these frequencies, the photodiode should see a loss in absorbed light, due to the absorption within this spectra. In other words, there will be an absorption loss upon transition between ν_1 and ν_2. The spacing between these are so close, however, that they are beyond the resolution to allow experimenters to distinguish them without further analysis.

A. Doppler broadening

A theoretical doppler broadening can be derived from Maxwell-Bolzman's velocity distributions of ideal gases:

$$P(V)dV = \sqrt{\frac{m}{2\pi k_B T}} e^{-mV^2/2k_B T}$$

Since we are interested in frequencies, we can convert the above equation by realizing that $V = \frac{c(f_L - f_0)}{f_0}$, where

f_L is the frequency of the light and f_0 is the resonance frequency of the atom at rest. So we can rewrite:

$$P(f_L)df_L = \frac{\sigma}{\sqrt{\pi}} e^{-\frac{(f_L - f_0)^2}{2\sigma^2}} dV_L$$

where $\sigma = \frac{f_0}{c}\sqrt{\frac{k_B T}{m}}$, thus predicting the FWHM to be: $2\sqrt{2ln(2)}\frac{f_0}{c}\sqrt{\frac{k_B T}{m}}$

In our setup we are working with red-infrared light ($f_0 \approx 384$THz) and room temperature (around 295K). Taking the Rb mass to be around 87.4678 atomic units predicts the Doppler broadening to be around 504.7 ± 2.0MHz, which will be a very important value for further analysis.

B. Hyperfine structure

For Rubidium, the spacing of hyperfine structure is less than the theoretical Doppler broadening at room temperature. As can be seen on Figure 4, the hyperfine spacing is on the order of 50-270MHz, while the theoretical Doppler broadening is around 504.7 MHz, which means that we will not be able to differentiate transitions. Therefore another technique must be implemented. Such technique is known as saturation spectroscopy. [2]

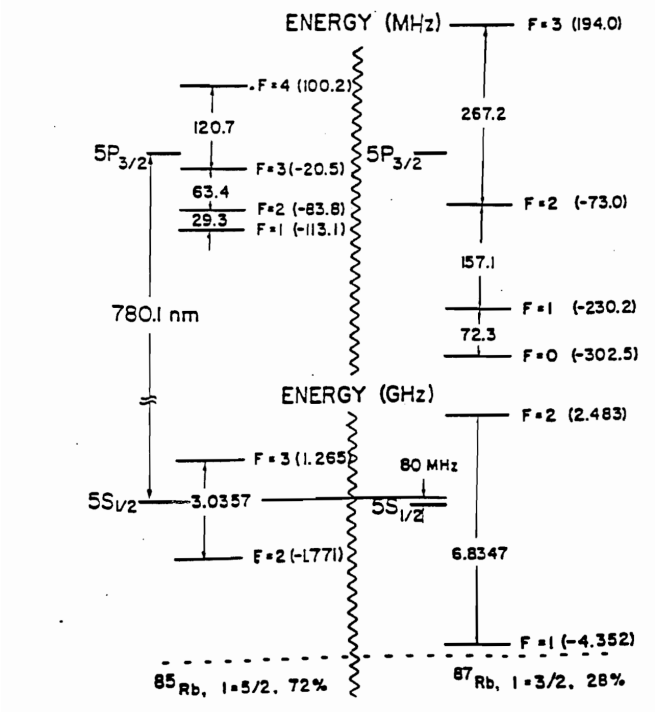

FIG. 4. Shows energy levels for the D2 line of rubidium.

In our setup, we send part of the laser beam (using a beam splitter) in the opposite direction to the initial path of the beam as shown in 2, which we will refer to as the saturating beam (and part that follows the original path, the initial beam). Since the saturating beam travels in the opposite direction, the doppler shifting in a sense goes in the opposite direction since the relative velocities of affected molecules are reversed. [2]

First, let's consider a case of a single transition (with the transition frequency, f_t). Let the laser span frequencies from $f_t - \Delta$ to $f_t + \Delta$. Notice then that for any frequency $f_t - \delta$ (with $0 < \delta < \Delta$) the absorption will only occur for molecules moving away with a corresponding velocity (call $v_{-\delta}$) as to compensate for the difference with the doppler shift. Notice also that the saturating beam sees these molecules shifted in another direction due to the opposite direction of the beam, therefore it will not saturate them. Similarly, the saturating beam with frequency $f_t + \delta$ will not affect the molecules moving with $v_{+\delta}$ velocity.

The above argument fails however if $\delta = 0$ and the laser is exactly at f_t frequency. In this case both the initial and the saturating beams see the stationary (near zero velocity) Rb molecules with zero doppler shift, which means that both beams will target the same excitement transitions. If the overall intensity of two beams is big enough, then the absorption will only be partial simply because there wouldn't be enough molecules to excite. Therefore we would expect to see very narrow doppler free peak at exactly f_t frequency.

C. Crossover peaks

In reality, we are usually dealing with many hyperfine transitions. In saturation spectroscopy this fact gives the rise to crossover peaks.

Crossover peaks appear when two transitions are within the Doppler broadening interval. Assume the two transition frequencies are $f_1 < f_2$, and let $f_m = \frac{1}{2}(f_1 + f_2)$ be the average frequency. Notice then that if the laser's frequency equals to f_m, and $\delta = f_m - f_1 = f_2 - f_m = \frac{1}{2}(f_2 - f_1)$, then molecules experiencing Doppler shift of δ (moving with either $v_{\pm\delta}$) will experience $\pm\delta$ Doppler shift from initial beam and $\mp\delta$ Doppler shift from the saturating beam. Since δ is chosen such that $f_1 + \delta = f_2 - \delta$, at f_m frequency both initial and saturating beams would excite a transition, therefore for big enough laser intensity we would again see a narrow Doppler free absorption gap peak.

More generally, we would expect to see a crossover peak for each transition pair at exactly the corresponding average frequency.

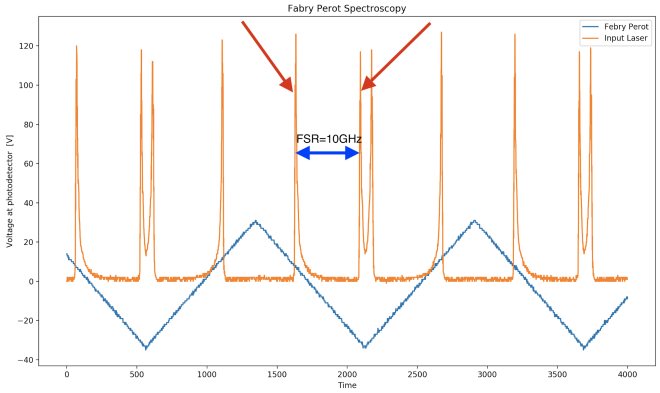

FIG. 5. Background Fabry Parot plot, which is used to convert change in time, Δt to change in frequency Δf. In our case 10GHz corresponds to 460 units in time (time between two shown peaks). Uncertainty due to the width of the peaks.

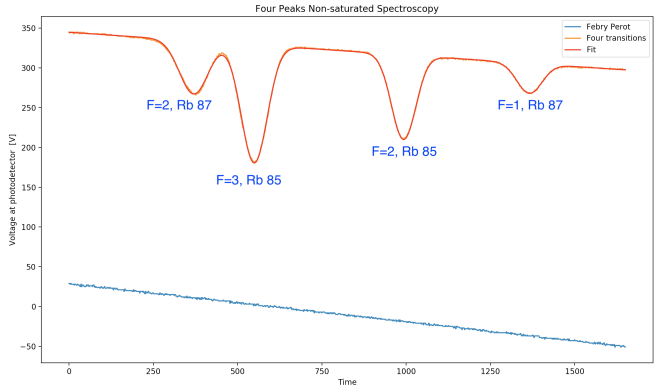

FIG. 6. Shows a region of non saturated spectrum of Rb with 4 labeled transitions of both Rb 85 and Rb 87 at the 780nm range. Additionally, a fit is shown (red) which simply is a superposition of a linear function and four gaussians for the background and each transition. Statistical uncertainty due to the uncertainty in fit parameters.

IV. MEASUREMENTS

A. Non-saturated

The data is fitted with a superposition of a linear function and four gaussians and takes a form:

$$f(x) = m \times x + b + \sum_{n=1}^{4} a_n exp(-\frac{1}{2}(\frac{x - c_n}{\sigma_n})^2) \qquad (1)$$

Such fit accounts for background intensity of a laser and the fine structure for each of the four transitions.

The fit from Fig. 6 produces parameters for four peaks:

TABLE I. Experimentally measured FWHMs and relative positions of centers.

Transition	Center* [GHz]	FWHM [GHz]	σ_{center}	σ_{fwhm}
F=2, Rb 87	31.9559	0.6940	0.0098	0.0261
F=3, Rb 85	33.2111	0.6352	0.0018	0.0047
F=2, Rb 85	36.3125	0.5881	0.0033	0.0080
F=1, Rb 87	38.8562	0.5775	0.0260	0.0636

*values of centers are relative, so are only used to find differences between centers not their actual values.

B. Saturated

Figure 7 shows the data collected for non-saturated and saturated F=1, Rb 87 peak. Due to a somewhat small resolution, averaging technique to reduce noise was applied (value at a point equals to the average of its neighbors). Once the data for saturated and non-saturated peak was obtained, the had to be calibrated.

In order to calibrate them Gaussian+linear (superposition of Gaussian and a line) fit was used for both (for saturated the middle part was excluded in the fit). Once fits were obtained, the difference in gaussian centers was used to adjust along x-axis and difference in the constant of linear part was used to adjust along the y-axis thus getting the Non-saturated adjusted curve which, as wanted, nearly matches the saturated curve everywhere except for the middle region.

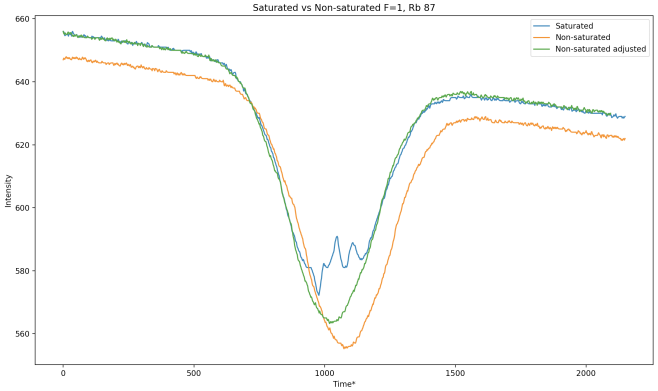

FIG. 7. Shows saturated vs non-saturated F=1, Rb 87 peaks. Also shows the required adjustment of non-saturated. Data noise has been slightly reduced using averaging technique. Statistical uncertainty due to the uncertainty in fit parameters and due to the fit region chosen approximately.

After the alignment, we can now look at the difference plot shown on Fig. 8. The peaks on the figure are manually annotated. The labels were assigned in accordance with the theoretical spacing of the transitions (70MHz between F'= 0,1 and 150MHz between F'=1,2). One crossover peak was also labeled for F'=1, 2.

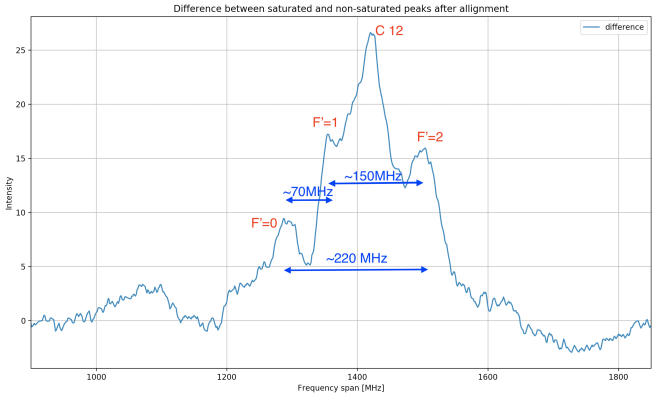

FIG. 8. Shows the difference between saturated and non-saturated F=1, Rb 87 peak alongside with manual labeling of peaks based on theoretical spacing and their strength (F'=1,2 peaks have save quantum coefficients of $\frac{5}{12}$ and therefore should have about the same height, while F'=0 has a smaller coefficient of $\frac{1}{6}$ and therefore a smaller height. Slight uncertainty due to resolution and smoothing. Main uncertainty comes from alignment on previous figure, since difference depends directly on them.

V. ANALYSIS

A. Saturation free

The most important thing to justify in this part is the choice of theoretical fit. Experimentally from Fig. 4, we can see that it is really good. The reason why linear+4gaussian fit makes sense goes as such. As we are spanning through frequencies, because we are doing it nearly linearly, the absorbed intensity should also vary linearly. This explains why we have the linear component. Now, since the distribution broadening occurs due to doppler broadening, and since the absorption is directly proportional to the number of molecules in the state, the expected absorption should also be Gaussian in accordance to Maxwell-Bolzman's velocity distribution equation. Finally, we can add them to get equation 1.

The first thing one can check is the frequency difference between first and last transitions (find the time difference between the peaks). This can be done simple by comparing the centers between the two peaks of the fit function in Fig. 6, which turns out to be $38.8562 - 31.9559 \approx 6.9003 \pm 0.0279 GHz$. Note that the actual value is around 6.8347 GHz and while doesn't fall within uncertainty interval is still very close.

As can be seen in the measurement section, the transition from F=1, Rb 87 has the largest FHWM and isn't coupled to other peaks, thus is best for the analysis. The measured FHWM for this peak is 0.5775 GHz, while the theoretical is 0.5047 GHz (for $f_0 = 384.0 THz$, 780nm laser). The difference in values can be partially explained by the hyperfine structure. According to theory, there are 3 possible transitions from F=1 to F'=0,1,2. The frequency spread of these 3 states is around 229 MHz = 0.229 GHz, which would widen the FWHM when taken into the account. Another potential source of error is the non-linearity of the time scale. So far we assumed that the laser spans the 10GHz interval in Fig. 5 linearly, meaning for example that a point in the middle between two peaks divides the interval in two 5 GHz segments. In reality, this assumption is only a good first approximation and, in fact, there is some decay in the span of frequencies which will be accounted for if the time permits.

1. *Second examination*

Upon second examination of the same set up, a difference value was found closer to 6.3 GHz. While at first such discrepancy was assumed to have been a result of wrong analysis (a new program was implemented to clean up the code), it was not the case since when it was ran on first data the same result was produced. The problem seems to lie in the physical setup of Fabry perot calibration. It is quite possible that another group has slightly adjusted the reflecting mirror preceding the Fabry perot which then shifted the calibration. It would make sense to attribute this discrepancy to a systematic error since not only it consistently produced lower frequency span, but also was only found upon a second examination several weeks after the first.

B. Saturated

After saturating the beam we focused on the change in the F=1, Rb 87 peak. As can be seen in Fig. 7 the saturated curve is in fact different from non-saturated. From a first glance one can notice several peaks, which are expected to be due to the hyperfine transition. What is really important however is to look at the difference. Since the curves were shifted, they first had to be adjusted. While this could be done manually, we have approached it more rigorously. Notice that both peaks resemble gaussian+linear shape (excluding the hyperfine portion). Therefore we could fit gaussian+linear fit into both saturated and non-saturated, then compare the fit parameters and adjust accordingly in order to align them, which is what is displayed as Non-saturated adjusted curve.

Once the alignment is performed, a difference is taken. Before displaying it, however, smoothing by averaging is applied (twice). Averaging does not affect the macroscopic properties, but only decreases the noise. The benefit can be seen from Fig. 9.

While all of the previous measurements were relatively closed to data, thus providing hope for a clear hyperfine structure, it, unfortunately is not exactly the result. While we definitely see peaks, we do not see 6 peaks (3 for each transition and 3 for each crossover pair). If we

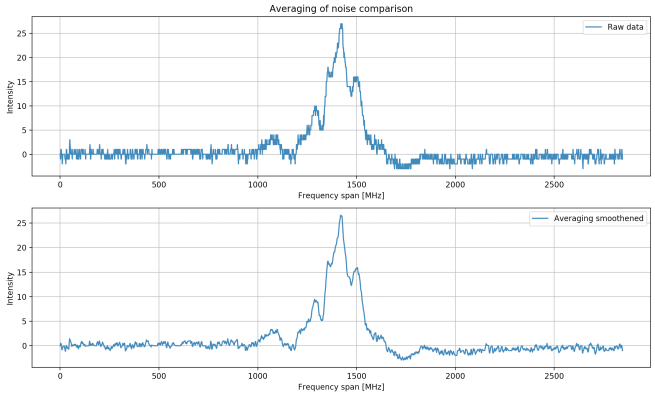

FIG. 9. Shows the difference data before and after averaging.

refer back to Fig. 4 we see that the crossovers and transition peaks are close to each other with spacing between peaks in order [MHz]: 36, 36, 38, 32, 70. Now adding the fact that our saturating beam wasn't going in the opposite direction and rather made an angle (around 10 degrees), we would expect the crossovers to shift. Given all that, it is possible that some of the crossovers coincide with other peaks or that labeling was not correct, but it is difficult to tell.

An argument for why our labeling was correct can be seen from the amplitudes of peaks. For our transition from F=1 to F'=0,1,2 we expect the transition occur in the ratios: $\frac{1}{6}, \frac{5}{12}, \frac{5}{12}$ [6, Table 8]. This seems to be the case as F'=1,2 peaks have about the same amplitude which is about 2-3 times bigger than the amplitude of F'=0 peak. Also the 1,2 crossover peak's amplitude is larger than the other two since there is twice as many affected molecules ($v_{\pm\delta}$) and the average is close to the transitions (relative to Dopler broadening of 504.7 MHz). This means that the crossover should have been about 1.5-2 times larger than the transition peaks.

C. Theoretical dopler broadening with hyperfine structure

As described in the Theory section, the dopler broadening of our laser at room temperature should be around 504.7 ± 0.2MHz, but the actual measured differ by quite a much (Table I). For example, for F=1, Rb 87 we get 577.5 ± 63.6 MHz. This in fact is not surprising due to the hyperfine structure. The measured fwhm is the fwhm of the superposition of Dopler broadening of each transition. Therefore the theoretical broadening should actually be different. We can improve the prediction by building a model where we take the hyperfine structure and then apply Dopler broadening to it. The result can be seen on Fig. 10.

The model predicts the FWHM of non-saturated peak to be 579.036 ± 0.007 MHz, compared to the actually measured width of 577.5 ± 63.6 MHz. Truly astonishing result! Well, there most likely was an element of luck since we did not include the crossover peaks, which would decrease the value. Regardless, we still have a much better prediction than the simple 504.7 MHz. The reader might be wondering why we are using the same theoretical Dopler broadening for all of these transitions, since they differ in terms of transition frequencies. The reason is that the since the original laser frequency is around 384THz, the difference in transition frequencies only produces a correction is 10th digit, which is obviously too small to be relevant.

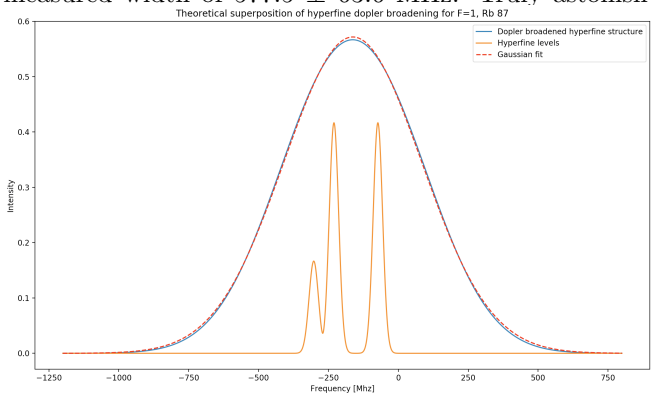

FIG. 10. Shows the theoretical superposition of Dopler broadened hyperfine structure. The FWHM of the fit is what we theoretically observe in non-saturated case. The model accounts for Clebsch-Gordan coefficients as can be seen in magnitude of Hyperfine levels.

VI. CONCLUSION

In this lab we have theoretically and experimentally demonstrated how the affects of Dopler broadening can be negated using saturation spectroscopy. We have shown how the hyperfine structure can be derived by comparing saturated and non-saturated data, then taking the difference and analyzing it. We have also described used numerical techniques, the most important one being gaussian+linear fit. We have also demonstrated how the hyperfine structure may give the rise to corrections in simple Dopler broadening, and discussed some of the further improvements that could be made to the model.

[1] J.-H. Wan, "Laser frequency locking based on the normal and abnormal saturated absorption spectroscopy of 87rb," (2016).
[2] D. W. Preston, "Doppler-free saturated absorption: Laser spectroscopy," (1996).
[3] S. U. of Technology, "Thermal doppler broadening," https://astronomy.swin.edu.au/cosmos/T/Thermal+Doppler+Broadening.
[4] U. of Florida — Department of Physics, "Saturated absorption spectroscopy," (2018).
[5] S. K. N. N. Martin Ebermann, Karla Hiller, "Design, operation and performance of a fabry-perot-based mwir microspectrometer," (2009).
[6] D. A. Steck, "Rubidium 87 d line data," (2001).